Received: 16 March 2021 | Revised: 31 May 2021 | Accepted: 1 June 2021

DOI: 10.1111/pce.14124

ORIGINAL ARTICLE

Plant, Cell & Environment WILEY

The size and the age of the metabolically active carbon in tree roots

Boaz Hilman[1] | Jan Muhr[1,2] | Juliane Helm[1] | Iris Kuhlmann[1] | Ernst-Detlef Schulze[1] | Susan Trumbore[1]

[1]Department of Biogeochemical Processes, Max-Planck Institute for Biogeochemistry, Jena, Germany

[2]Department of Bioclimatology, Georg-August University Göttingen, Göttingen, Germany

Correspondence
Boaz Hilman, Department of Biogeochemical Processes, Max-Planck Institute for Biogeochemistry, Jena, Germany.
Email: bhilman@bgc-jena.mpg.de

Funding information
H2020 European Research Council, Grant/Award Numbers: 682512, 695101

Abstract

Little is known about the sources and age of C respired by tree roots. Previous research in stems identified two functional pools of non-structural carbohydrates (NSC): an "active" pool supplied directly from canopy photo-assimilates supporting metabolism and a "stored" pool used when fresh C supplies are limited. We compared the C isotope composition of water-soluble NSC and respired CO_2 for aspen roots (*Populus tremula* hybrids) cut off from fresh C supply after stem-girdling or prolonged incubation of excised roots. We used bomb radiocarbon to estimate the time elapsed since C fixation for respired CO_2, water-soluble NSC and structural α-cellulose. While freshly excised roots (mostly <2.9 mm in diameter) respired CO_2 fixed <1 year previously, the age increased to 1.6–2.9 year within a week after root excision. Freshly excised roots from trees girdled ~3 months ago had respiration rates and NSC stocks similar to un-girdled trees but respired older C (~1.2 year). We estimate that over 3 months NSC in girdled roots must be replaced 5–7 times by reserves remobilized from root-external sources. Using a mixing model and observed correlations between $\Delta^{14}C$ of water-soluble C and α-cellulose, we estimate ~30% of C is "active" (~5 mg C g^{-1}).

KEYWORDS
fine roots, girdling, isotopic fractionation, nonstructural carbohydrates, phosphoenolpyruvate carboxylase (PEPC), radiocarbon (^{14}C), respiration, storage dynamics, tree carbon dynamics, $\delta^{13}C$

1 | INTRODUCTION

Fine root (≤ 2 mm) biomass is estimated at 40.8 Pg C globally, about 7% of total vegetation carbon (C) (Ciais et al., 2014; Jackson, Mooney, & Schulze, 1997). The proportion of C allocated belowground for growth, respiration, exudation, root connection and mycorrhizal associations are larger, 25–63% of assimilated C in forest ecosystems (Litton, Raich, & Ryan, 2007). These functions are concentrated in fine (typically <1 mm diameter) roots that respire the highest C per unit mass (Pregitzer, Laskowski, Burton, Lessard, & Zak, 1998), conduct root exudation and mycorrhizal interactions and have high mass turnover rates (Gaudinski et al., 2010). Nonstructural carbohydrates (NSC, mostly soluble sugars and starch) are known to fuel these functions with C and energy. Stored NSC reserves can support cellular functions when current C supply is insufficient (Chapin III, Schulze, & Mooney, 1990; Dietze et al., 2014).

The "bomb-radiocarbon" approach permits quantification of respiration sources and NSC dynamics in mature trees by tracing excess ^{14}C created during atmospheric nuclear weapons tests that nearly doubled background values of radiocarbon signature ($\Delta^{14}C$) of

atmospheric CO_2 ($\Delta^{14}C_{atm}$) in the early 1960s (Trumbore, Sierra, & Pries, 2016). Since then, decline in $\Delta^{14}C_{atm}$ reflect uptake of bomb-radiocarbon into the oceans and terrestrial biosphere, and dilution by radiocarbon-free CO_2 originating from fossil fuel emissions (Levin & Hesshaimer, 2016). Since 1964, an annual unique $\Delta^{14}C_{atm}$ signature is transferred to biomass C via photosynthesis. A comparison of the $\Delta^{14}C$ signature of any C pool in plants to the current year's $\Delta^{14}C_{atm}$ thus provides a means to estimate the mean time elapsed since the C was fixed.

Plants use soluble sugars both to transport C (predominantly sucrose) and as primary substrates in cellular metabolism (e.g. glucose and fructose). Starch is insoluble and thus cannot be translocated but can serve as local storage. These different properties are often mistakenly implied to reflect differences in turnover time, with sugars are assumed to comprise a fast-cycling pool and starch a slow-cycling pool (Dietze et al., 2014). However, in tree stems and large roots no systematic differences in radiocarbon signatures have been observed between the water-soluble (representing sugars) and insoluble (starch) C fractions, suggesting fast C exchange between the two pools (Richardson et al., 2013; Richardson et al., 2015; Trumbore, Czimczik, Sierra, Muhr, & Xu, 2015).

Nevertheless, NSC pools are not uniform in age. The $\Delta^{14}C$ of stem respired CO_2 ($\Delta^{14}C_{resp}$) was lower than the water-soluble $\Delta^{14}C$ ($\Delta^{14}C_{ws}$) in the outermost 2 cm of the stem, reflecting age differences of ~10 year (Carbone et al., 2013). Combined with evidence from ^{13}C-labelling of fresh photo-assimilates from the canopy, it is clear that some young sugars support respiration, while other, older, sugars are stored intact (Epron et al., 2011). Accordingly, C allocation models usually distinguish two functional NSC-sub pools: a "fast" pool of recently fixed C (assumed age < 1 year) supporting metabolism and respiration, and a "slow" NSC pool for storage (Herrera-Ramirez et al., 2020; Richardson et al., 2015). However, we are still missing ways to quantify and differentiate between these two pools.

Measuring $\delta^{13}C$ can provide information about the substrate and the metabolic pathways in respiration. Variations in the $\delta^{13}C$ signature of produced sugars are primarily controlled by photosynthetic fractionation at the leaf level (Farquhar, Oleary, & Berry, 1982). "Post-photosynthetic fractionations" during transport, biosynthesis, and respiration further modify $\delta^{13}C$ signatures (Badeck, Tcherkez, Nogues, Piel, & Ghashghaie, 2005; Ghashghaie et al., 2003; Werner & Gessler, 2011). Starch is usually slightly enriched (~1‰) while lipids are more depleted (~ −5‰) in ^{13}C compared to sugars (Bowling, Pataki, & Randerson, 2008), and are expected to accordingly affect the $\delta^{13}C$ signature of the respired CO_2 ($\delta^{13}C_{resp}$) when decarboxylated. The "apparent isotopic fractionation" of respiration (Δ_R) is defined as the difference in $\delta^{13}C$ between the putative respiratory substrate (usually sugars) and $\delta^{13}C_{resp}$ (Ghashghaie et al., 2003). For roots of woody C_3 plants mainly negative Δ_R values ($\delta^{13}C_{substrate} < \delta^{13}C_{resp}$) have been reported (Ghashghaie & Badeck, 2014). The ^{13}C enrichment in respired CO_2 is commonly explained by the dominance of CO_2 emitted from decarboxylation of pyruvate via pyruvate dehydrogenase (PDH) over CO_2 emitted from the tricarboxylic acid (TCA) cycle reactions (Tcherkez et al., 2003). The activity of phospho*enol*pyruvate carboxylase (PEPC), which re-fixes CO_2 to replenish TCA cycle intermediates, was suggested to decrease respired CO_2 enrichment and increase Δ_R (Gessler et al., 2007; Ghashghaie & Badeck, 2014). To our knowledge, only one study to date has evaluated Δ_R in roots of mature trees (Gessler et al., 2007).

Here, we investigated the sources of respiration for fine and coarse roots of mature temperate aspen trees (*Populus tremula* hybrids). We performed a stem-girdling experiment (complete circumferential removal of bark, cambium, and phloem), terminating below-ground transport of fresh photo-assimilates and forcing mobilization of storage NSCs for survival beneath the girdling. Girdled Amazonian tree stems quickly shifted from using current year photosynthetic products as respiratory substrates in un-girdled trees to C fixed ~5 year previously a month after girdling (Muhr, Trumbore, Higuchi, & Kunert, 2018). We expected increases in $\Delta^{14}C_{resp}$ for roots of girdled trees, but with potentially smaller magnitude, since trees from the genus *Populus* often have root connections that enable C transfer from healthy trees (Gaspard & DesRochers, 2020; Pregitzer & Friend, 1996). To characterize the usage of NSC reserves in the roots themselves we conducted additional experiments where the age of C respired from detached roots was followed for a week. This experiment is also the base for our first approach to estimate the size and isotopic signature of the fast-cycling "active" C pool that feeds respiration and metabolism. The relationship between $\Delta^{14}C_{ws}$ and the $\Delta^{14}C$ signature of the α-cellulose ($\Delta^{14}C_{cell}$, representing structural C) allowed us to develop the second approach to estimate the size and isotopic signatures of the "active" C, as well as the slow-cycling "stored" C pool.

2 | MATERIALS AND METHODS

2.1 | Study site and experimental design

We sampled 12 Eurasian aspen trees (*Populus tremula* hybrids) with estimated age of 60–70 year growing in a forest stand located on a slope of the Großer Hermannsberg Mountain (867 m a.s.l), Germany (50°42′50″ N, 10°36′13″ E, site elevation 616 m a.s.l). Soils at the site are developed on volcanic parent rock, mean annual temperature is ~7°C and annual rainfall is 800–1,200 mm (Bouriaud, Marin, Bouriaud, Hessenmoller, & Schulze, 2016). During our field campaign in the summer of 2018, an extreme "hot drought" occurred in central Europe (Bastos et al., 2020), also observed in a nearby weather station situated 812 m a.s.l (https://www.bgc-jena.mpg.de/freiland/index.php/Sites/Hermannsberg). During the 2018 growing season (May and October), mean monthly temperatures were warmer by 1.5–3.5°C than those for the years 2010–2017, while total monthly rainfall was 260 mm, compared to the average of 323 mm in the years 2010–2017 (Figure 1).

The size of the forest stand where our study took place is ~40 × 40 m^2 with ca. 20 mature and 50 younger trees. Control and girdled trees were all mature with diameter at breast height of 87–129 cm, and interspersed. Distances between girdled trees and the

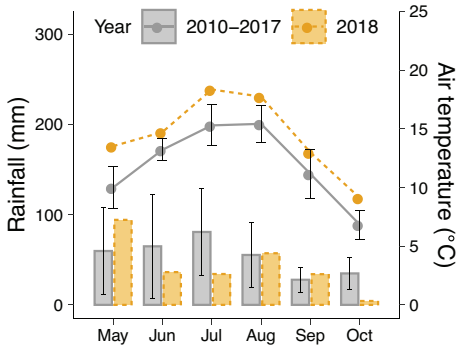

FIGURE 1 Mean monthly rainfall (mm, bars) and air temperature (°C, circles) during 2018 growing season, and in the previous 8 years (2010–2017) in the study site (Großer Hermannsberg, Germany). Error bars for the 2010–2017 data represent one standard deviation from the mean [Colour figure can be viewed at wileyonlinelibrary.com]

closest un-girdled trees, including unstudied trees, were 1.2–5.8 m. After sampling all 12 trees on 26 June and 4 July, six of the trees were girdled on July 4th by removing a ~4 cm wide band of bark, cambium and phloem from the stem 1.5 m above the ground. During subsequent samplings (25 September and 2 October), we differentiated "Girdling" and "Control" trees.

To ensure we sampled roots specific to the chosen trees, we tracked their connections back to the main root or stem. Roots were collected from the top 10 cm of the mineral soil. We aimed at finding two root clusters for each tree with total mass of several grams. In most trees, we harvested individual roots growing directly from large lateral roots to gain the desired mass. Hence, a sample from a single tree usually combined roots from several spatial locations. The samples were put on ice immediately after harvest until analysis. On the subsequent day, the roots were thoroughly washed to remove any remaining soil particles and then separated into two size classes: coarse roots (> 2 mm, mean 2.9 mm, max 6 mm) and fine roots (≤ 2 mm, almost all were suberized); each size fraction consisted of roots from different orders, and not necessarily from the same root cluster. Each size class was split for (a) NSC and α-cellulose extractions, and (b) respiration incubations (details below).

Incubations of excised roots lasted for 2 days and integrated CO_2 respired between the start of incubation (time 0) to day 2. To test roots' ability to utilize their own C reserves for metabolism during C starvation, we made additional incubations that sampled integrated respiration between days 6 and 8. We report these using the mean incubation times (e.g., days 1 and 7). In addition, we performed short-term incubations (up to 1.5 hr) on days 0, 2 and 6 to measure the respiratory quotient (RQ), that is, the ratio CO_2 efflux/O_2 influx. The RQ is mainly defined by the respiratory substrate, which in plants is assumed to be carbohydrates with RQ = 1. Compounds more oxidized than carbohydrates like organic acids are expected to yield RQ > 1, whereas amino acids and lipids yield RQ values of 0.9 and 0.7, respectively (Masiello, Gallagher, Randerson, Deco, & Chadwick, 2008). Thus, RQ measurements can indicate the substrate used for respiration. For the correction of CO_2 efflux rates measured at laboratory temperatures (22°C) to field temperatures, we conducted short-term incubations at different temperatures to calculate Q_{10}, the factor by which CO_2 efflux increases with 10°C warming.

Because regional fossil fuel emissions have the potential to affect $\Delta^{14}C_{atm}$, we collected additional samples at the site to reconstruct the recent history of local $\Delta^{14}C_{atm}$ from tree rings. Two stem cores from nearby tree were extracted in 2019 using a 5.15 mm increment borer. We visually identified the annual rings for the last 9 years and sampled their outermost halves, which presumably are dominated by latewood produced during midsummer-autumn mainly from C fixed in the current growing season, thus approximating the current year's $\Delta^{14}CO_{atm}$ (Kudsk et al., 2018; Pilcher, 1995). Samples from identical rings from both stem cores were pooled for α-cellulose extraction and $\Delta^{14}C_{cell}$ analysis (Hoper, McCormac, Hogg, Higham, & Head, 2016). In addition, assuming leaves respire C fixed recently, we analysed $\Delta^{14}C_{resp}$ from aspen leaves as a proxy for $\Delta^{14}C_{atm}$ during the 2019 growing season. We combined our data with the mean $\Delta^{14}C_{atm}$ of the northern hemisphere zone 1 during the growing season (May–October) as published by Hua, Barbetti, and Rakowski (2016). We further compared our estimation for 2018 $\Delta^{14}C_{atm}$ with direct measurements of atmospheric air in different sites in Europe that are part of ICOS (the Integrated Carbon Observation System, see Table S1 for PID numbers).

2.2 | NSC analysis

Aliquots of 50 mg oven-dried root tissue (≥2 d at 60°C), were analysed for (a) sugars and starch concentrations, (b) $\Delta^{14}C_{ws}$, (c) $\delta^{13}C_{ws}$, and (d) $\Delta^{14}C_{cell}$. Since $\Delta^{14}C_{ws}$ is usually correlated with the age of the containing tissue (Furze et al., 2020; Richardson et al., 2015; Trumbore et al., 2015), for correct interpretation of $\Delta^{14}C_{ws}$ variance it is important to account to the root's mean C age estimated using $\Delta^{14}C_{cell}$. Therefore, we coarsely cut rather than milled the roots since in the α-cellulose extraction the sample is rinsed with reagents through 16–40 μm mesh that might allow fine material to pass and clog the system's tubing (Steinhof, Altenburg, & Machts, 2017). We decided only after the pre-girdling campaign to measure starch concentration, hence data are available only for roots from the girdled and control trees.

The methods for NSC, sugar and starch extractions are based on protocols S1 and S2 from Landhausser et al. (2018) with some modifications necessary for minimizing extraneous C additions that would affect the ^{14}C measurement. We avoided plastic vials that contain C and used only glass vials that were pre-baked at 550°C to eliminate any C residuals. For sugar extraction we used water as a solvent instead of ethanol, which is slightly more efficient (Landhausser et al., 2018), to avoid possible C addition from the ethanol. To reduce starch dissolution in water, the extraction temperature was lowered from 90°C to 65°C. Extraction of water-soluble C from the 50-mg samples was carried out by shaking the samples in 5 ml deionized water for 10 min (65°C), in three repetitions. After each repetition the vials were cooled, centrifuged and the supernatant was transferred to

a glass vial kept on ice (to slow-down microbial degradation). A subsample of 2 ml from the total 15 ml was used for quantification of the sugars sucrose, glucose and fructose. For the $\delta^{13}C$ and $\Delta^{14}C$ analysis, the rest of the solution was concentrated by freeze-drying and pipetted into tin capsules for $\delta^{13}C$ analysis, and into pre-baked silver capsules for $\Delta^{14}C$ analysis. The starch in the pellet from the water extraction was converted by α-amylase (Sigma cat. no. A4551) into water-soluble glucans and then to glucose by amyloglucosidase (Sigma cat. no. ROAMYGLL) (Landhausser et al., 2018). The remaining pellet was used for $\Delta^{14}C_{cell}$ analysis (Steinhof et al., 2017).

To measure the concentrations of the soluble sugars and the glucose hydrolysate from the starch digestion we used high-performance anion-exchange chromatography with pulsed amperometric detection (HPLC-PAD) device equipped with autosampler (Dionex® ICS 3000, Thermo Fisher GmbH, Idstein, Germany) (Raessler, Wissuwa, Breul, Unger, & Grimm, 2010). The starch and sugar concentrations are calculated as glucose-equivalent weight per sample dry weight (mg glucose g^{-1}) (Landhausser et al., 2018), and further multiplied by 0.4 to express as C mass per dry weight (mg C g^{-1}).

2.3 | Respiration measurements

2.3.1 | Two-day incubations

Root samples (0.3–1.2 g dry weight) were incubated in gas-tight Plexiglas cylinders equipped with fittings (12.7 mm Swagelok Ultra-Torr) on each side for attaching sampling flasks (115 ml) equipped with a Louwers™ O-ring high-vacuum valve (LouwersHanique, Hapert, Netherlands) (Muhr et al., 2018). Total system volume was 269 ± 10 ml. Before incubation, the headspace containing the washed roots was flushed with synthetic air (0% CO_2, 20% O_2) for 3 min in order to remove any inherited CO_2. Then the set-up was closed quickly by connecting two flasks (pre-filled with the same synthetic air) at both ends of the chamber. Incubations were conducted at room temperature (22°C) in the dark and ended by closing the flask valves. Leaf incubations aimed to estimate the local $\Delta^{14}CO_{atm}$, used the same setup and lasted 1 day.

Incubations were conducted at room temperature that was higher than average field soil temperatures. While direct effects on substrate identity and thus age ($\Delta^{14}C_{resp}$) are not expected initially, higher temperatures could lead to faster depletion of "fast" sources and thus ageing of the substrate pools, expected to affect both $\Delta^{14}C_{resp}$ and $\delta^{13}C_{resp}$ (Tcherkez et al., 2003). In addition, the temperature-induced metabolic change can affect $\delta^{13}C_{resp}$ directly reflecting temperature sensitivity of the processes emitting CO_2 (Kodama et al., 2008). Thus, the $\delta^{13}C_{resp}$ values should be regarded as room-temperature acclimated values and not extrapolatable to field values.

2.3.2 | Short-term incubations

Short-term incubations were done in a solid aluminium chamber equipped with an NDIR CO_2 sensor (COZIR 0%–1% CO_2 Sensor, CO_2Meter, Inc., Ormond Beach, FL) and a quenching-based O_2 sensor (LuminOx, Coatbridge, UK). CO_2 and O_2 fluxes were calculated by linear fit of the concentration change with time, where the slope is equivalent to the term $\Delta CO_2/I_t$ in Equation (2). Incubations with $R^2 < 0.9$ in any of the gases were discarded.

Flask-measured CO_2 efflux rates (measured at room temperature) were corrected to field (in situ) temperatures using Q_{10} values estimated using incubations of roots collected in the September–October at two or three different temperatures (ranging between 5°C and 22°C). We used the R package *respirometry* that fits the measured CO_2 efflux (R) at a given temperature (T) with the Equation $R = a \times e^{b \times T}$ and calculates $Q_{10} = e^{10 \times b}$. We assume the computed Q_{10} value is also valid for the June–July campaign following Burton and Pregitzer (2003) who observed little to no seasonal temperature acclimation in fine roots. Soil temperature in the top 10 cm where the roots were collected is coupled to changes in air temperature with some lag time (Brown, Pregitzer, Reed, & Burton, 2000). To estimate air temperature at the site we added 1.6°C to the measured temperature at the weather station due to altitude difference (196 m) and assumed mean lapse rate of 0.8°C every 100 m. Soil temperature (0–10 cm) was estimated as the average air temperature over the previous 7 days.

2.4 | Radiocarbon analysis

For radiocarbon analysis, respired CO_2 from the flasks or CO_2 from combusted solid samples was cryogenically purified and graphitized on iron in the presence of H_2 at 550°C (Muhr et al., 2018; Steinhof et al., 2017). The graphitized samples were analysed by accelerator mass spectrometry (AMS; Micadas, Ionplus, Switzerland) in the radiocarbon laboratory in Jena, Germany (Steinhof et al., 2017). Radiocarbon data are expressed as $\Delta^{14}C$ (‰) and calculated according to Trumbore et al. (2016):

$$\Delta^{14}C = \left[\frac{R_{-25}}{0.95 \times R_{oxalic,-19} \times e^{x-1950}/8267}\right] \times 1{,}000, \quad (1)$$

where R_{-25} is the sample's $^{14}C/^{12}C$ ratio corrected for mass dependent fractionation by normalizing the sample's $\delta^{13}C$ to a $\delta^{13}C$ of −25‰. $R_{oxalic,-19}$ is the $^{14}C/^{12}C$ ratio in the standard, oxalic acid, normalized to $\delta^{13}C$ of −19‰, and the 0.95 term converts to the absolute radiocarbon standard (1890 wood) activity in 1950. The exponent corrects for decay of ^{14}C in the standard between 1950 and the year of measurement (x), to provide the absolute amount of ^{14}C in our samples. For individual tree rings x matched the estimated year.

The measurement precision for each AMS measurement of ^{14}C was 2–3‰. The estimated mean age of measured C is calculated from the difference between its $\Delta^{14}C$ value and the $\Delta^{14}C_{atm}$ during the 2018 growing season, divided by the mean annual decline in $\Delta^{14}C_{atm}$ (see Equation [5] in Results).

Our samples were assumed to have $\Delta^{14}C \geq \Delta^{14}C_{atm}$, therefore, samples with $\Delta^{14}C < \Delta^{14}C_{atm}$ were considered contaminated with extraneous fossil C. One batch of nine samples was discarded due to many results with highly negative values.

2.5 | CO_2 efflux rate and $\delta^{13}C$ analysis

The CO_2 concentration and $\delta^{13}C$ in the two-day incubations were determined from a sub-sample of air from one flask analysed by Isotope Ratio Mass Spectrometer (IRMS; Delta+ XL; Thermo Fisher Scientific) coupled to a modified gas bench with Conflow III and GC (Thermo Fisher Scientific, Bremen, Germany). Air from the flask was expanded into a pre-evacuated 12-ml Labco extainer (Labco Ltd, Lampeter, UK) equipped with a septum cap. Argon gas (Ar) was added to the exetainer to create a small over pressure to enable passive sampling by the auto-sampler (CTC Combi-PAL autosampler, CTC-Analytics, Zwingen, Switzerland). The air pressure values in the exetainer before and after the Ar addition were recorded for pressure correction. Each exetainer was sampled twice (30 or 50 μl per aliquot) by the auto-sampler and the aliquots were injected into the IRMS. Samples were analysed against a laboratory air standard on the Vienna Pee Dee Belemnite (VPDB) scale [Jena Reference Air Set-06 (JRAS-06), (Wendeberg, Richter, Rothe, & Brand, 2013)]. For estimating the CO_2 concentration the m/z peaks 44, 45 and 46 were integrated and calibrated against samples of standard gas with a known concentration of 2,895 ppm. $\delta^{13}C_{resp}$ and CO_2 concentration were determined from the mean of two sequential injections. For $\delta^{13}C_{resp}$ the mean standard deviation (SD) of the duplicate samples was 0.04‰. For CO_2 concentration the mean SD for the duplicate samples was 14 ppm, regardless of the samples' concentration.

We tested the CO_2 concentration evaluation using the calibrated IRMS peak area by analysing flasks filled with known CO_2 concentrations using the same IRMS measurement protocol and found the IRMS overestimated CO_2 concentration by 4% at 10,000 ppm and 18% at 50,000 ppm. Empirical corrections based on a polynomial fit were used to correct reported sample concentrations. After correction, differences between known to corrected CO_2 concentrations were 0% on average and for 90% of the measurements the difference was < 2% of the measured concentration. In the same test, we found that the $\delta^{13}C$ was stable when varying the injection volume up to 200 μl and in flask air pressures between 800 and 1,000 hPa, suggesting there are no isotopic fractionations in the sub-sampling procedure.

The mean CO_2 efflux during the incubation period normalized to the sample dry weight per day (mg C g^{-1} day^{-1}) was calculated using Equation (2):

$$CO_2\ \text{Efflux} = \frac{\Delta CO_2}{I_t} \times \frac{V_{HS} \times BP \times M_C}{T \times M_{dm} \times R}, \quad (2)$$

where ΔCO_2 is the net change in CO_2 concentration (ppm/10^6) during the incubation (equal to the measured CO_2 concentration), I_t is the incubation time (days), V_{HS} is the volume of the headspace (269 ml), BP is the local barometric pressure (hPa), M_C is the molar mass of C (12 mg $mmole^{-1}$), T is the temperature of incubation (295°K), M_{dm} is the dry mass of roots (g) and R is the ideal gas constant (83.14 ml hPa k^{-1} $mmol^{-1}$). The error in the CO_2 efflux due to propagated uncertainties in ΔCO_2, V_{hs}, BP and M_{dm} is estimated to be 4% of the reported value.

To measure $\delta^{13}C_{ws}$, the capsule containing water-soluble C was combusted using an elemental analyser (NA 1110, CE Instruments, Milan, Italy) coupled to a Delta$^+$XL IRMS (Thermo Finnigan, Bremen, Germany) via a ConFlow III. Samples were analysed against laboratory standards on the VPDB scale.

The apparent isotopic fractionation (Δ_R, ‰) in respiration was estimated with the equation (neglecting the denominator):

$$\Delta_R = \delta^{13}C_{ws} - \delta^{13}C_{resp}. \quad (3)$$

2.6 | Estimations of C pool sizes and age

The first approach (approach 1, Table 1) is based on the view that storage C age follows "last in, first out" dynamics (Lacointe, Kajji, Daudet, Archer, & Frossard, 1993), in which the most recent C transported to the root is the most accessible for respiration (Carbone et al., 2013). Accordingly, two pools were defined: (a) an "active" pool that supports metabolism and respiration, derived from recently transported C to the roots (in intact roots under no C limitation, recently fixed C < 1 year), and (b) a "stored" pool that only becomes active when the supply of transported C is reduced (Figure 2) (Herrera-Ramirez et al., 2020; Richardson et al., 2013). We measured respired CO_2 as a proxy to estimate the age and size of the metabolically "active" pool, with $\Delta^{14}C_{resp}$ representing its age. To estimate the amount of storage C < 1 year old (the active pool size in intact roots) we used the repeated respiration measurements. First, C with $\Delta^{14}C$ signature of 1 year was defined as the 2018 $\Delta^{14}C_{atm}$ + the mean yearly $\Delta^{14}C_{atm}$ change (see Equation [5] in Results). Assuming excised roots will access increasingly older (higher $\Delta^{14}C$) C, we estimated when the CO_2 respired by the roots increased beyond this 1 year threshold ($t_{depletion}$). Integration of the fitted CO_2 efflux versus time curve between time = 0 until $t_{depletion}$ yielded an estimate of the size

TABLE 1 Methods for C pool size and age estimation

	Approach 1: Respired CO_2 analysis	Approach 2: Water-soluble C and α-cellulose analysis
Stored C fraction (F_{stored})		Slope
Active C fraction (F_{active})		1 − slope
$\Delta^{14}C_{stored}$		$\Delta^{14}C_{cell}$
$\Delta^{14}C_{active}$	$\Delta^{14}C_{resp}$	Intercept/F_{active}
Size of active pool	Amount of respired CO_2 that is < 1 year	Total sugars × F_{active}
Size of stored pool		Total sugars × $F_{passive}$

Note: Approach 1 is based on the $\Delta^{14}C$ signature of root-respired CO_2 ($\Delta^{14}C_{resp}$), and approach 2 is based on the intercept and slope estimates of the fitted linear line between the $\Delta^{14}C$ signatures of the water-soluble C ($\Delta^{14}C_{ws}$) and α-cellulose C ($\Delta^{14}C_{cell}$) extracted from roots. Those C extractions represent soluble sugars and structural C, respectively.

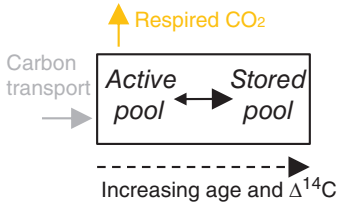

FIGURE 2 Conceptual model indicate the carbon (C) dynamics in a root, represented by the box. Carbon transported into the root is the most accessible to metabolism and respiration, while a portion is allocated to the stored pool. The $\Delta^{14}C$ signature of respired CO_2 is assumed to be equal to the transported C signature. When photosynthesis is not suppressed the transported C has $\Delta^{14}C$ signature of current atmospheric CO_2. Respired CO_2 older than 1 year might originate from stored pool C, or from transported C translocated from root-external old storage. The $\Delta^{14}C$ of the total sugars, approximated by $\Delta^{14}C_{ws}$, is the weighted age of the young active pool and the older stored pool [Colour figure can be viewed at wileyonlinelibrary.com]

of the "active" pool of C younger than 1 year in intact roots. This approach is indifferent to the actual storage compound that supports respiration.

Our second approach (approach 2, Table 1) is based on the strong correlation between $\Delta^{14}C_{ws}$ and tissue age and the observation that $\Delta^{14}C_{ws}$ is often less than (younger) than $\Delta^{14}C_{cell}$ (Furze et al., 2020; Richardson et al., 2015; Trumbore et al., 2015).

For a root that has lived for multiple years, we expect that $\Delta^{14}C_{cell}$ will reflect the ^{14}C of substrates used for growth that can vary from year to year, while the $\Delta^{14}C_{ws}$ will reflect mixing of C that may date from the year of root formation with soluble C translocated from other parts of the plant. The mean $\Delta^{14}C_{ws}$ signature of a root thus comprises a spectrum of $\Delta^{14}C$ values, ranging from recently assimilated C in young tissues to older storage C in the innermost ring. Hence, in simplified view, the measured $\Delta^{14}C_{ws}$ is a weighted mean of the two functional C fractions (Figure 2): a proportion of active C, F_{active}, with radiocarbon signature $\Delta^{14}C_{active}$ and the stored fraction C, F_{stored} (= 1 – F_{active}), with radiocarbon signature $\Delta^{14}C_{stored}$. The mass balance is described by (Equation [4]):

$$\Delta^{14}C_{ws} = F_{active} \times \Delta^{14}C_{active} + F_{stored} \times \Delta^{14}C_{stored}. \quad (4)$$

We assume that the stored pool C consists of C deposited as storage reserves concurrent with root growth, thus $\Delta^{14}C_{stored}$ can be approximated by the measured $\Delta^{14}C_{cell}$. Even if old C with high $\Delta^{14}C$ signature is allocated to a root, the formed structural C and storage C are expected to share the high isotopic signature and the assumed approximation will still hold. Using the linear regression estimates for the relation between the measured $\Delta^{14}C_{ws}$ with $\Delta^{14}C_{cell}$ enables us to solve the other variables of Equation (4); The slope of the linear equation is equal to F_{stored}, F_{active} equals 1 – F_{stored} and the intercept equals to $F_{active} \times \Delta^{14}C_{active}$, thus $\Delta^{14}C_{active}$ = intercept/F_{active}. Using this approach, we do not assume an age for the active C (e.g., < 1 year); instead, we estimate the $\Delta^{14}C$ of F_{active} from the $\Delta^{14}C_{ws}$ value that is not explained by $\Delta^{14}C_{cell}$. The model estimates are based on roots from different trees hence they represent averaged values for several trees (n = 5–12).

It is important to note that the water-soluble fraction contains sugars, but also many other soluble compounds like tannins and amino and organic acids. Trumbore et al. (2015) estimated that ~50% of the C in the soluble fraction extracted from wood (they used methanol: water mixture as a solvent) originates from the sugars sucrose, glucose and fructose. Here, we assume that on timescales of > 1 year exchange of C between cellular metabolites means that the $\Delta^{14}C_{ws}$ signature approximates that of sugars.

2.7 | Statistical analysis

All data were analysed using *R* (*R* Core Team, 2019). We tested effects of treatment (Pre-girdling, girdling and control) and root class (coarse, fine) on the different measures. Normality was tested with the Shapiro–Wilk test and equality of variance with Leven's test. When both assumptions were not violated we proceed with one or two-way ANOVA followed by Tukey's HSD post-hoc test. When the assumptions of normality and/or homogeneity were violated, we used the non-parametric Kruskal–Wallis rank-sum test, followed by pairwise Wilcoxon Rank Sum Tests. For the linear models, we used the *lm* function.

3 | RESULTS

3.1 | NSC concentrations

Total sugar concentrations did not vary by treatment (p = .91, Kruskal-Wallis) or root size class (p = .91, ANOVA) (Figure 3a). The overall mean ± SE (n = 47) was 42.9 ± 3.1 mg glucose g^{-1} dry root, equivalent to 17.1 ± 1.2 mg C g^{-1} (Table S2). The mean composition of the C (in glucose equivalents) was: sucrose 69.4%, glucose 16.6% and fructose 14.0%. Starch measured in girdling and control treatments was significantly higher (p = .04, Kruskal-Wallis) in the coarse roots than in the fine roots, with mean values of 4.8 ± 1.2 and 1.5 ± 0.3 mg C g^{-1}, respectively (n = 12).

3.2 | CO_2 efflux rate

The CO_2 efflux rate in the two-day incubations was significantly higher in the fine roots than in the coarse roots (p < .01, Kruskal-Wallis) with mean ± SE values of 3.0 ± 0.3 and 2.0 ± 0.2 mg C g^{-1} d^{-1}, respectively (Figure 3b). The mean Q_{10} measured in September–October campaigns was 2.3 ± 0.1 (n = 11) with no effect of root class or treatment. Correcting the CO_2 efflux rates measured in the laboratory to soil temperature decreased the values, but the root size effect remained significant (p < .01, Kruskal-Wallis), with mean values of 1.2 ± 0.1 and 0.8 ± 0.1 mg C g^{-1} d^{-1} were assessed for the fine and

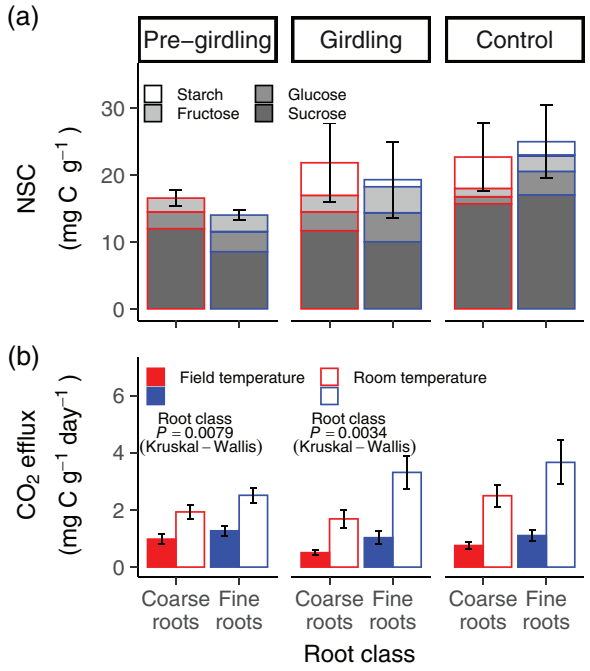

FIGURE 3 Means ± SE of coarse (> 2 mm) and fine (2 ≤ mm) roots collected before girdling (Pre-girdling), ~3 months after girdling (Girdling) and ~3 months after girdling but in un-girdled trees (Control). (a) NSC concentrations separated by molecules. Starch was not measured in pre-girdling roots. $n = 11, 12, 6, 6, 6, 6$, respectively; (b) CO_2 efflux rates measured in two-day incubations in room temperature (empty bars) and corrected to field temperature (full bars). $n = 10, 11, 6, 6, 6, 6$, respectively. Below the legends the respective significant statistical tests [Colour figure can be viewed at wileyonlinelibrary.com]

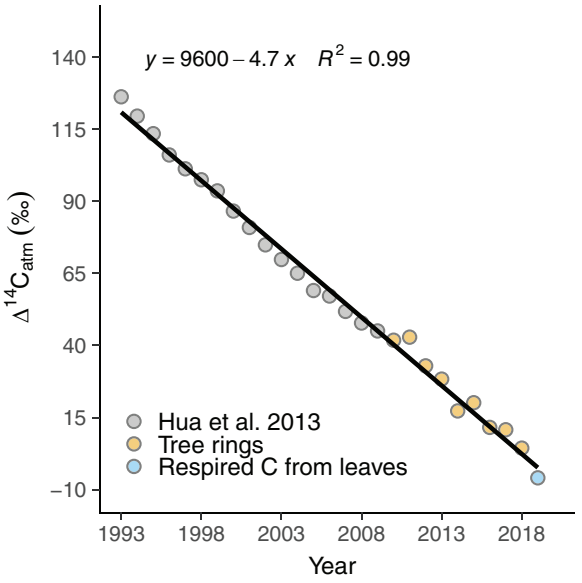

FIGURE 4 The estimated atmospheric $\Delta^{14}C$ signature ($\Delta^{14}C_{atm}$) in the study site during the last two decades. The atmospheric record in grey is the mean $\Delta^{14}C_{atm}$ of the northern hemisphere zone 1 after Hua et al. (2016). Tree rings in orange is the α-cellulose $\Delta^{14}C$ signature measured for the late wood in annual rings from years 2010 to 2018. The blue point is the $\Delta^{14}C$ signature of respired CO_2 from leaves harvested in July 2019, which assumed to represent recent photo-assimilates thus current $\Delta^{14}C_{atm}$. The linear equation indicates the mean annual decline in $\Delta^{14}C_{atm}$ is 4.7‰ [Colour figure can be viewed at wileyonlinelibrary.com]

$$\text{Mean age} = \frac{\Delta^{14}C - 2.3‰}{4.7‰/\text{year}}. \quad (5)$$

coarse roots, respectively (Figure 3b). We used the mean efflux rates corrected to the daily mean of soil temperature to estimate the total amount of C respired by fine and coarse roots during the 82 days between the girdling and the first post-girdling campaign; these were 150 ± 19 and 100 ± 12 mg C g^{-1}, respectively (uncertainty was calculated by varying the mean efflux rates and Q_{10} with their uncertainties). Accordingly, the mean daily C respired in the fine roots is 1.8 ± 0.2 mg C g^{-1} and 1.2 ± 0.1 mg C g^{-1} in the coarse roots.

3.3 | Radiocarbon

Combining measures of $\Delta^{14}C_{cell}$ in tree-ring late wood, leaf $\Delta^{14}C_{resp}$ and the atmospheric record in the region, the annual decline of $\Delta^{14}C_{atm}$ averaged 4.7‰ per year during the last two decades (Figure 4). Our estimate for the atmospheric $\Delta^{14}C_{resp}$ during the 2018 growing season was +2.3‰, the mean $\Delta^{14}C_{resp}$ of the roots of the control trees (Table 2). This value is within the 0.6–4.4‰ range of $\Delta^{14}C_{atm}$ mean values measured during the 2018 growing season at several ICOS stations (Table S1). Thus, we calculated the mean age (year) of a C pool with radiocarbon signature $\Delta^{14}C$ using Equation (5):

Root respired $\Delta^{14}C_{resp}$ values were mostly similar to the $\Delta^{14}C_{atm}$ in the year of collection, with overall mean ± SE of 4.8 ± 0.9 (0.5 ± 0.2 year; $n = 36$) and range of −5.2‰ to +23.7‰ (0–4.6 years). The mean $\Delta^{14}C_{resp}$ when both root classes are pooled together was higher in the girdled trees (7.9 ± 1.9; $n = 12$) than the pre-girdling (4.2 ± 0.8; $n = 12$) and the control (2.3 ± 1.8, $n = 12$) (Figure 5). Differences between the treatments were not significant ($p = .14$–$.20$, Wilcoxon). However, the mean $\Delta^{14}C_{resp}$ of the girdled trees was significantly higher than the control trees (represent current atmosphere) when compared exclusively ($p = .04$, Wilcoxon). The mean age of the respired $\Delta^{14}C_{resp}$ in the girdled trees was 1.2 ± 0.4 year, compared to 0 ± 0.4 year in the control roots.

The $\Delta^{14}C_{ws}$ values were higher than $\Delta^{14}C_{resp}$ for the same root samples, ranging between 0.8 and 90.7‰ (0–18.8 year). The linear regression model equations for the $\Delta^{14}C_{ws}$ versus $\Delta^{14}C_{cell}$ relationship, its statistical information and approaches 1 and 2 predictions are presented in Table 2 and Figures 5 and 6. The variability in $\Delta^{14}C_{cell}$ explained the majority of the variability in $\Delta^{14}C_{ws}$ ($r^2 > 0.8$ in most groups; Table 2; Figure 6). The slope estimates based on the linear fit equations were highly significant in most subgroups ($p < .01$), except in the fine roots of the girdled trees due to one outlier with much higher $\Delta^{14}C_{ws}$ than $\Delta^{14}C_{cell}$ (Figure 6). According to approach 2, F_{stored}

TABLE 2 A summary of approaches 1 and 2 results

Treatment	Root class	Measured $\Delta^{14}C_{resp}$ and age[a] ($\Delta^{14}C_{active}$ estimation of approach 1)		Linear model equations[b]		F_{stored}, F_{active}[c]		$\Delta^{14}C_{active}$ and age[d] (estimation of approach 2)	
Pre-girdling	Coarse	5.2 ± 1.9‰ (0.6 ± 0.4 year, $n = 6$)	4.2 ± 1.1‰ (0.4 ± 0.2 year)	$y = -4.4\,(3.7) + \mathbf{0.8}x\,(0.1)$ $r^2 = 0.88$, $df = 9$	$y = -0.3\,(2.5) + \mathbf{0.7}x\,(0.1)$ $r^2 = 0.79$, $df = 21$	0.8, 0.2	0.7, 0.3	−23.0 ± 22.8‰ (−5.4 ± 4.9 year)	−1.1 ± 8.8‰ (−0.7 ± 1.9 year)
	Fine	3.2 ± 1.0‰ (0.2 ± 0.2 year, $n = 6$)		$y = 3.8\,(3.6) + \mathbf{0.6}x\,(0.1)$ $r^2 = 0.64$, $df = 10$		0.6, 0.4		9.1 ± 9.1‰ (1.4 ± 1.9 year)	
Girdling	Coarse	8.25 ± 3.2‰ (1.3 ± 0.7 year, $n = 6$)	7.9 ± 1.9‰ (1.2 ± 0.4 year)	$y = 3.1\,(2.7) + \mathbf{0.7}x\,(0.04)$ $r^2 = 0.99$, $df = 4$	$y = 5.5\,(4.7) + \mathbf{0.7}x\,(0.1)$ $r^2 = 0.84$, $df = 10$	0.7, 0.3	0.7, 0.3	11.0 ± 9.6‰ (1.9 ± 2 year)	17.5 ± 15.8‰ (3.2 ± 3.4 year)
	Fine	7.5 ± 2.3‰ (1.1 ± 0.5 year, $n = 6$)		$y = 15.8\,(18.1) + 0.4x\,(0.6)$ $r^2 = 0.1$, $df = 4$		0.4, 0.6		25.2 ± 36.8‰ (4.9 ± 7.8 year)	
Control	Coarse	0.7 ± 2.0‰ (−0.3 ± 0.4 year, $n = 6$)	2.3 ± 1.8‰ (0 ± 0.4 year)	$y = \mathbf{4.0}\,(1.0) + \mathbf{0.55}x\,(0.03)$ $r^2 = 0.99$, $df = 3$	$y = \mathbf{4.8}\,(1.4) + \mathbf{0.6}x\,(0.05)$ $r^2 = 0.93$, $df = 9$	0.55, 0.45	0.6, 0.4	9.0 ± 2.2‰ (1.4 ± 0.5 year)	11.3 ± 3.5‰ (1.9 ± 0.7 year)
	Fine	3.8 ± 3.0‰ (0.3 ± 0.6 year, $n = 6$)		$y = 4.0\,(2.9) + 0.\mathbf{66}x\,(0.13)$ $r^2 = 0.86$, $df = 4$		0.7, 0.3		11.8 ± 9.9‰ (2.0 ± 2.1 year)	
All		4.8 ± 0.9 (0.5 ± 0.2 year)			$y = 1.7\,(1.7) + \mathbf{0.7}x\,(0.05)$ $r^2 = 0.84$, $df = 44$	0.7, 0.3		5.7 ± 5.9‰ (0.7 ± 1.3 year)	

Note: The linear model equations are for the relationship between the $\Delta^{14}C$ signatures of the water-soluble C ($\Delta^{14}C_{ws}$) and α-cellulose C ($\Delta^{14}C_{cell}$) extracted from roots. Those C extractions represent soluble sugars and structural C, respectively. Approach 2 is based on the linear model and predicts the fractions of the stored (F_{stored}) and active (F_{active}) C pools from the total water-soluble C, and the $\Delta^{14}C$ signature of the active pool ($\Delta^{14}C_{active}$).

[a]Values are means ± SE.

[b]Bold numbers indicate significant ($p < .05$) estimate of the model. The standard errors of the coefficients are in parentheses.

[c]The error is the model's slope SE, F_{stored} equals the equation's slope, $F_{active} = 1 - F_{stored}$.

[d]Calculated as the equation's intercept/F_{active}. Errors are the propagated standard errors of the intercept and slope estimates.

equals the fitted line slope, hence the overall F_{stored} (± SE of the model) is 0.7 ± 0.05 and values in the subgroups range between 0.55 ± 0.03 and 0.8 ± 0.1 (without the exceptional girdled fine roots). The overall F_{active}, which equals 1 – F_{stored}, is 0.3 with range of 0.2–0.45 in the subgroups. Significant intercept estimates were computed only for the coarse roots and coarse + fine roots of the control trees ($p < .05$), while in the other subgroups the errors were rather large (Table 2). The uncertainties in $\Delta^{14}C_{active}$ estimations (= Intercept/F_{active}) are also large as a result of the propagation of the intercept errors. The overall $\Delta^{14}C_{active}$ calculated by approach 2 is 5.7 ± 5.9‰ with an estimated age of 0.7 ± 1.3 year (Table 2).

Among the measured C pools the $\Delta^{14}C_{cell}$ values were the highest and ranged between 2.6 and 123.6‰ (0–25.8 years). Coarse roots had higher mean $\Delta^{14}C_{cell}$ (34.4 ± 5.9‰; $n = 23$; 6.8 ± 1.3 year) than fine roots (24.0 ± 2.7‰; $n = 24$; 4.6 ± 0.6 year), but the relation was not statistically significant ($p = 0.40$, Kruskal-Wallis).

3.4 | Repeated incubations

Temporal changes in all measured parameters were observed between day 1 and day 7 of the repeated incubations (Figure 7). Mean $\Delta^{14}C_{resp}$ (± SE) increased more rapidly in the fine roots (from 3.2 ± 0.8 to 16.1 ± 2.1‰) than in the coarse roots (from 4.4 ± 0.3 to 10.1 ± 0.9‰), corresponding to estimated ages of 2.9 ± 0.5 and 1.6 ± 0.2 year (Figure 7a) at the end of incubation, respectively. The CO_2 efflux rates declined over time, but remained higher in fine roots compared to coarse roots (Figure 7b).

Following approach 1, any carbon with $\Delta^{14}C < 7‰$ [the sum of $\Delta^{14}C_{atm}$ (2.3‰) and annual decline (4.7‰)] was defined as younger than 1 year. Using linear regression, we estimated that the 7‰ value was exceeded after 2.3 and 4.3 days (= $t_{depletion}$) in fine and coarse roots, respectively, indicating time to deplete the active C pool (Figure 7a). Integrating the total CO_2 efflux over time (fitted curves in Figure 7b) between time = 0 and time = $t_{depletion}$ gives an estimate of the active pool size: 5.3 and 5.1 mg C g^{-1} for fine and coarse roots, respectively. The total amount of C respired over the 7 days of incubation was calculated as 13.4 and 7.1 mg C g^{-1} for fine and coarse roots, respectively, which is equivalent to 66 and 35% of the total mean NSC-C in fine and coarse roots, respectively.

The $\delta^{13}C$ of CO_2 respired by coarse-roots ($\delta^{13}C_{resp}$) did not change between the first (−27.40 ± 0.16‰) and second incubation (−27.36 ± 0.06‰), while RQ decreased from 0.90 ± 0.15 to 0.65 ± 0.06 (Figure 7c,d). Over the same time period the $\delta^{13}C_{resp}$ for fine roots decreased by 0.83‰ (−27.53 ± 0.09 to −28.35 ± 0.12) and RQ declined to an even greater degree than in the coarse roots, from 1.08 ± 0.08 to 0.55 ± 0.06.

3.5 | $\delta^{13}C$ results

The $\delta^{13}C$ of the water soluble fraction extracted from roots varied significantly with treatment ($p < .001$; two-way ANOVA) and root

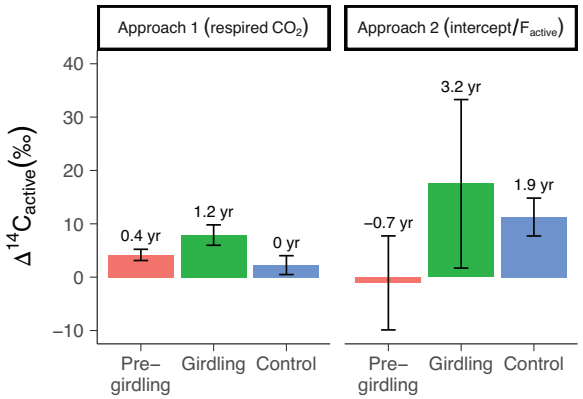

FIGURE 5 The $\Delta^{14}C$ signatures and mean age estimations of the active C pool according to two approaches; approach 1 assumes $\Delta^{14}C_{active}$ equals to the $\Delta^{14}C$ signature of respired CO_2 ($\Delta^{14}C_{resp}$); approach 2 is based on the intercept and slope estimates of the fitted linear line between the $\Delta^{14}C$ signatures of the extracted water-soluble C ($\Delta^{14}C_{ws}$) and α-cellulose C ($\Delta^{14}C_{cell}$). According to this approach the fraction of the active C pool $F_{active} = 1 - slope$. Roots collected before girdling (Pre-girdling), ~3 months after girdling (Girdling) and ~3 months after girdling but in un-girdled trees (Control). One set of roots was used for respiration incubations ($n = 12$) and second set was used for the C extractions ($n = 23$, 12, 11, respectively). Error bars of approach 1 is the standard errors of the $\Delta^{14}C_{resp}$ results, and of approach 2 are the cumulative standard errors of the slope and intercept estimates [Colour figure can be viewed at wileyonlinelibrary.com]

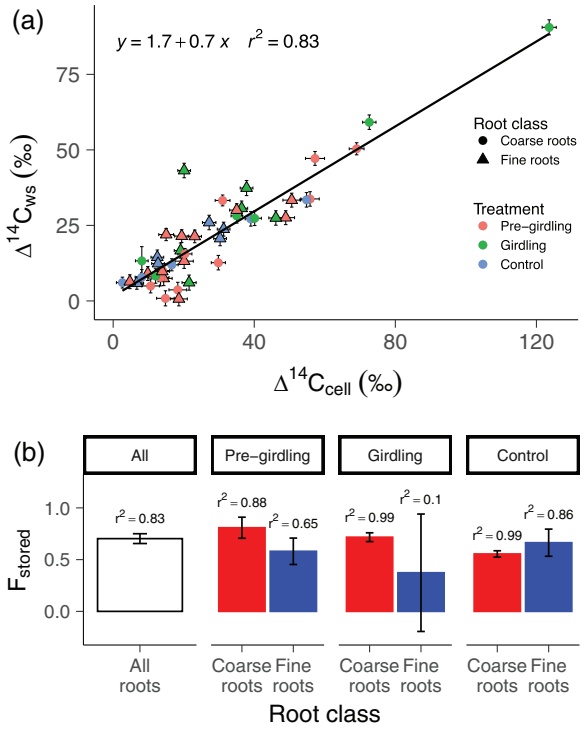

FIGURE 6 (a) A scatter plot of the $\Delta^{14}C$ signatures of the water-soluble C ($\Delta^{14}C_{ws}$) and α-cellulose C ($\Delta^{14}C_{cell}$) extracted from roots, with the equation of the linear model for all results pooled together. The shapes indicate the root class (coarse roots, > 2 mm, fine roots, ≤ 2 mm), and colours indicate the treatment: before girdling (Pre-girdling), ~3 months after girdling (Girdling) and ~3 months after girdling in un-girdled trees (Control). Error bars are the analitycal uncertainty; (b) the stored fraction (F_{stored}) from the total water-soluble C as estimated from the slope when the linear model is applied to the different subgroups ($n = 46, 11, 12, 6, 6, 5, 6$, respectively). For example, the slope in the equation in panel (a) is 0.7 therefore F_{stored} for the subgroup "All" is 0.7. Labels within the bars are the r^2 of the linear regression. Error bars are the standard error of the slope estimate [Colour figure can be viewed at wileyonlinelibrary.com]

size ($p < .01$), with no interaction effect ($p = .833$) (Figure 8a, Table S2). The post-hoc tests (Tukey's HSD) showed $\delta^{13}C_{ws}$ in the pre-girdling roots were significantly lower than the girdling and control roots that did not differ significantly. Water soluble C extracted from fine roots was 0.74‰ more enriched than the coarse root extracts. The treatment had significant effect also for $\delta^{13}C_{resp}$ ($p < .001$, Kruskal-Wallis), and the post-hoc test (Wilcoxon) indicates significant difference between all three campaigns: the pre-girdling roots had the lowest mean value, with girdled trees on average 1.15‰ higher and the control trees 2.64‰ higher than the pre-girdling (Figure 8b, Table S2). The coarse root $\delta^{13}C_{resp}$ was 0.80‰ more enriched than the fine roots ($p = .052$, Kruskal-Wallis). The mean Δ_R value ($\delta^{13}C_{ws} - \delta^{13}C_{resp}$) for fine roots was 1.53‰ higher than for coarse roots ($p < .01$; one-way ANOVA; Figure 8c). The treatment had marginal effect ($p = .053$; Kruskal-Wallis), where the Δ_R in the control roots was significantly lower (wilcoxon test) than in the pre-girdling and girdling (Figure 8c, Table S2).

4 | DISCUSSION

4.1 | Size and age estimates for active and stored C pools using two approaches

Our results provide unique estimates for the size and age of the functional sub-pools of NSC soluble in water using two distinct approaches. The correlation between $\Delta^{14}C_{ws}$ and $\Delta^{14}C_{cell}$ (approach 2) suggests that the C stored over multiple years on average makes up 70 ± 5% (range of 55–80%) of the extracted, water-soluble C (Figure 6). Sugars make up only a fraction of the water-soluble C used for the $\Delta^{14}C_{ws}$ measurement. Assuming sugars contribute in the same proportion to both active and stored pools found in water-soluble C, of the total average sugar concentration (17.1 ± 1.2 mg C g^{-1}; Table S2), 30% (5.1 ± 0.5 mg C g^{-1}) is found in the active pool and 70% (12.0 ± 0.5 mg C g^{-1}) in the stored pool (Table 1; approach 2). Based on the amount of C respired in repeated incubations (approach 1), we estimated the pool of C younger than 1 year as 5.1 mg C g^{-1} for coarse roots and 5.3 mg C g^{-1} for fine roots. Both approaches thus agree well in estimating the active pool size, suggesting that the < 1 year criterion provides a way to estimate the age and size of the active pool in intact roots. Both approaches (1 and 2) also agree with regard to the active pool age being younger than 1 year, that is, 0.5 ± 0.2 and 0.7 ± 1.3 year, respectively (Table 2). Our results in roots

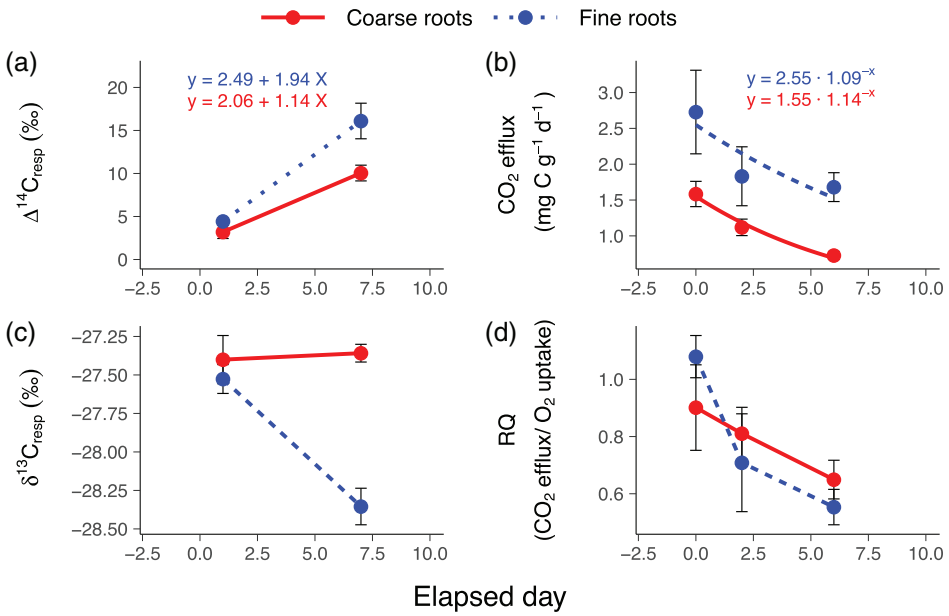

FIGURE 7 Results (mean ± SE) for coarse roots (> 2 mm) and fine roots (≤ 2 mm) from repeated respiration incubations during 7 days. (a) the $\Delta^{14}C$ signature of the respired CO_2 ($\Delta^{14}C_{resp}$). Presented are equations of linear regression models; (b) CO_2 efflux rates. Presented are equations that best fitted the results to the equation $y = a \times b^{-x}$; (c) the $\delta^{13}C$ signature of respired CO_2 ($\delta^{13}C_{resp}$); (d) RQ (ratio CO_2 efflux/O_2 uptake). Results in panels (a) and (c) were measured in two-day flask incubations ($n = 4$, 3 for coarse and fine roots, respectively), results in panels (b) and (d) were measured in short-term incubations (~20 min, according to the consecutive incubations order, $n = 3$, 4, 3 for coarse roots, and $n = 3$, 4, 4 for fine roots) [Colour figure can be viewed at wileyonlinelibrary.com]

corroborate those found by Richardson et al. (2013) for tree stems. When they constrained active ("fast") NSC pool age to < 1 year, they found this pool contributed 23–56% of the total NSC, compared with our estimates of 20–45% for roots (Table 2).

We also found disagreements between the two approaches, namely for individual subgroups (Figure 5, Table 2). There are apparently two reasons. The first reflects large uncertainties in the linear model's prediction of the intercept value that approach 2 is based on, which leads to extreme and unrealistic $\Delta^{14}C_{active}$ values, for example, equivalent to −5.4 year for coarse roots during pre-girdling (Table 2). Still, considering the uncertainties, the two approaches to estimate $\Delta^{14}C_{active}$ mostly agree (Figure 5). In addition, the tendency to use older C to fuel respiration (i.e., transferring older C to the active pool) in the girdled-trees roots that were predicted and observed in approach 1 ($\Delta^{14}C_{resp}$), was also observed in approach 2 (Figure 5).

The second source for the disagreement between the methods is potentially true difference, as apparent for the control roots, where the estimate from approach 2 for $\Delta^{14}C_{active}$ (based on the $\Delta^{14}C_{ws}$ that is not explained by variability in $\Delta^{14}C_{cell}$) is significantly higher than approach 1 considering the uncertainties (Figure 5, Table 2). A change in the age of the incoming C to the roots during the recent past might have impact on that discrepancy. Further understanding would require better estimation of the composition of water soluble components and the potential for their makeup and age to change with season.

4.2 | The stored fraction should be also considered in driving Δ_R values

Water deficit in the soil increased from midsummer to the end of the growing season because of the 2018 hot drought conditions (Figure 1). In control (un-girdled) trees, we observed enrichment in both $\delta^{13}C_{ws}$ and $\delta^{13}C_{resp}$ measured in Sept/Oct compared to the pre-girdling roots measured in June–July. These $\delta^{13}C_{resp}$ increases are in line with expected water shortage effects on leaf-level fractionation (Figure 8) (Farquhar & Sharkey, 1982; Madhavan, Treichel, & Oleary, 1991; Pate & Arthur, 1998; Scartazza, Moscatello, Matteucci, Battistelli, & Brugnoli, 2015). Smaller enrichments in $\delta^{13}C_{ws}$ could be explained by dilution with storage pools. A simple mass balance calculation using the relative enrichments in $\delta^{13}C_{ws}$ (+1.12‰) and $\delta^{13}C_{resp}$ (+2.64‰) between control and pre-girdling provides an estimate for F_{active}: 1.12/2.64 = 0.42, nearly equalling the 0.43 predicted by approach 2 for the control trees (Table 2). This suggests that ^{13}C-enriched sugars produced in control-tree leaves are mixed into the active pool in the roots where they support respiration, while the stored water-soluble C integrates more depleted $\delta^{13}C$ values inherited from previous years. Thus the apparent decrease in Δ_R in the control roots most likely does not reflect a metabolic shift (e.g., reduced PEPC activity) in the roots. In contrast, the enrichment between pre-girdled and girdled roots is larger for $\delta^{13}C_{ws}$ (+1.52‰) than for $\delta^{13}C_{resp}$ (+1.15‰), perhaps reflecting differences in transported substrates.

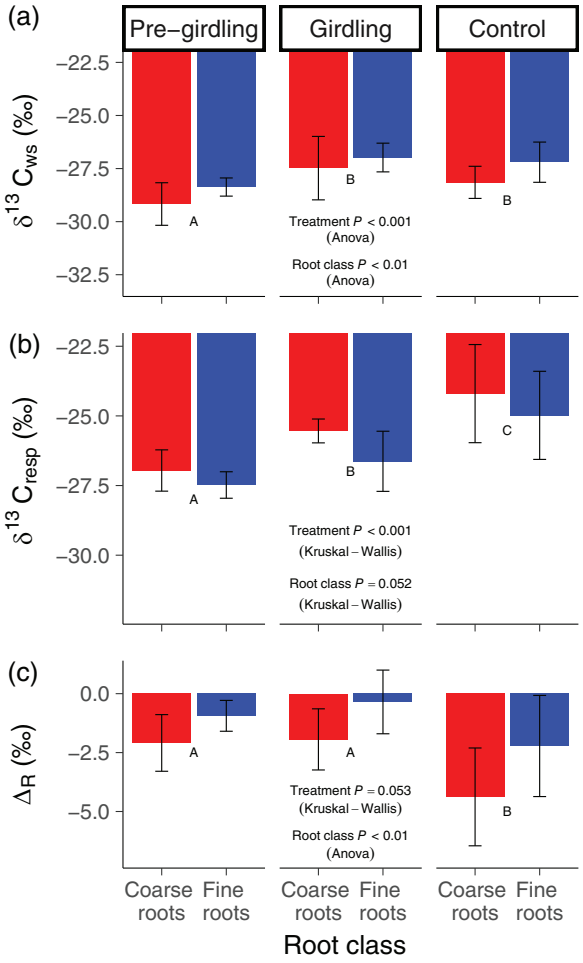

FIGURE 8 Means ± SE of coarse (> 2 mm) and fine (≤ 2 mm) roots collected before girdling (Pre-girdling), ~3 months after girdling (Girdling) and ~3 months after girdling in un-girdled trees (Control). (a) the $\delta^{13}C$ signature of the water-soluble C ($\delta^{13}C_{ws}$). According the order from left to right $n = 10, 11, 6, 6, 5, 6$; (b) the $\delta^{13}C$ signature of the respired CO_2 ($\delta^{13}C_{resp}$). According the order from left to right $n = 9, 10, 6, 6, 6, 6$; (c) the apparent fractionation factor ($\Delta_R = \delta^{13}C_{ws} - \delta^{13}C_{resp}$). According to the order from left to right $n = 7, 9, 6, 6, 5, 6$. Letters indicate significant differences between groups [Colour figure can be viewed at wileyonlinelibrary.com]

4.3 | The carbon balance in girdled-tree roots was maintained by translocation of stored NSC

The ability of roots to access older C for respiration when new C supply is cut off was demonstrated in the repeated incubations and in the girdling experiments. However, the supply of older C was not the same in both cases. Over the 7 days of the repeated incubations, the coarse and fine roots respired 7.1 and 13.4 mg C g^{-1}, respectively, roughly 35–70% of the 20.3 mg C g^{-1} of NSCs contained in the incubated roots (overall sugars and starch mean, Table S2). The estimated ages of the respired C increased from < 1 year to 1.6 and 2.9 year, for coarse and fine roots, respectively. This is consistent with roots respiring an initial active pool fed by freshly fixed C and switching to older substrates as this pool is exhausted (Herrera-Ramirez et al., 2020). In the case of excised roots, the source of the older C substrate was clearly in the roots themselves.

During the months that elapsed after girdling, root respiration rates did not decline as they did for excised roots (Figure 3b). During this period, assuming constant respiration rates, an estimated 100 and 150 mg C g^{-1} were respired in the coarse and fine roots, respectively. This was roughly 5–7 times higher than the C stored in the NSC pools, which also did not decline following girdling (Figure 3a). Therefore, it is clear that the C being respired in the girdled roots must be replaced by C translocated from root-external sources. The C may originate from storage in below-girdling parts of the tree, and from neighbouring healthy trees. *Populus* trees are known to have root connections with shared root systems. *Populus* root systems can remain functional for at least 20 year after shoot removal, and can persist for millennia while shoots are repeatedly resprouting (Pregitzer & Friend, 1996). Thus, the root systems of our girdled trees may be older than the ~60–70 year stems and have disproportionally large NSC stocks with possible connection from girdled to healthy trees. Natural root grafting, the phenomena where two roots are pressed together to form vascular continuity that enables C transfer between trees, is also common in *Populus* trees and could be a source for the replenished C (Fraser, Lieffers, & Landhausser, 2006; Gaspard & DesRochers, 2020; Mudge, Janick, Scofield, & Goldschmidt, 2009). Carbon transfer from neighbouring trees can occur also via mycelial networks (Rog, Rosenstock, Korner, & Klein, 2020). Indeed, the girdled trees in our study have survived for 2 years so far without visible signs of crown damage. Tree responses to girdling vary with species, stand age and experimental design that affect the size of the storage reserves and the connections between non-girdled and girdled trees (Levy-Varon, Schuster, & Griffin, 2012). The fact that our girdled trees were located among the un-girdled trees without physical or substantial spatial separation increase the chances for C sharing via roots. A way to reduce such effects in future is to girdle trees as a block of forest stand and isolate from root connections by trenching at the border.

Whatever the source of translocated C to girdled tree roots, our isotopic measurements indicate that it is not derived from fresh photo assimilates. Based on $\Delta^{14}C_{resp}$, the mean age of C respired from girdled roots was ~1.2 year older than C respired from control roots (Figure 5). This is younger than the respired C at the end of the repeated incubations (1.6–2.9 year). Difference in the $\delta^{13}C_{resp}$ between the girdling and control roots further indicates they do not share the same respiratory C source (Figure 8b). The increase in $\delta^{13}C_{resp}$ between pre-girdling and girdling can be explained by hydrolysis of starch, which tends to be more enriched than sugars (Brugnoli, Hubick, von Caemmerer, Wong, & Farquhar, 1988; Damesin & Lelarge, 2003; Gleixner, Danier, Werner, & Schmidt, 1993; Maunoury-Danger et al., 2010).

4.4 | Hints for high PEPC activity in the fine roots

The Δ_R mean values by root class and treatment ranged between (−0.35‰) and (−4.38‰) (Figure 8, Table S2), a slightly wider range

than the (−0.7‰) to (−3.1‰) values measured in mature Eucalypt roots (Gessler et al., 2007). While some of this could be due to differences in temperature effects, these likely do not explain the range in Δ_R values. As discussed earlier, the driver for the most negative Δ_R values measured in the control trees probably reflects differences in $\delta^{13}C$ between the active and the stored C pools ("mixing"), and not a change in respiration metabolism (Figure 8). In fact, it is difficult to resolve whether the main driver for a given Δ_R value is mixing or metabolism, especially in perennial plants with old reserves. However, differences in metabolism might be inferred in some circumstances, for example when comparing Δ_R in fine and coarse roots from the same trees where uniform mixing could be assumed. Δ_R was higher for fine (−1.1‰) than coarse (−2.67‰) roots, a difference reflecting lower $\delta^{13}C_{resp}$ (−0.80‰) and higher $\delta^{13}C_{ws}$ (+0.74‰) in the fine roots (Figure 8). This pattern is in agreement with the expected net isotopic effect of refixation of internal CO_2 by PEPC: a ^{13}C depletion of the respired CO_2 and a ^{13}C enrichment of the products (Werner & Gessler, 2011).

Additional support for CO_2 fixation with high PEPC activity in roots comes from the decline in the respiration quotient (RQ) from ~1 to ~0.6 during our repeated incubations (Figure 7d), since PEPC CO_2 re-fixation would reduce CO_2 efflux and thereby RQ (Hilman et al., 2019). The effect of PEPC on respiration grows as its activity as a fraction of total respiration increases (Badeck et al., 2005), as might occur with repeated incubations. Our results mirror those of Bathellier et al. (2009) who also observed a decrease in RQ from 1.1 to 0.8–0.9 while $\delta^{13}C_{resp}$ remained stable in roots of French bean during 6 days of carbohydrate starvation by darkening. Alternative explanations for the change in RQ exist, including a shift from carbohydrates to lipids as the main respiration substrate (Figure 7d). However, we observed no simultaneous decline in $\delta^{13}C_{resp}$ that would be expected to accompany such a substrate shift, given the depleted $\delta^{13}C$ value of lipids (Fischer et al., 2015; Tcherkez et al., 2003). Other factors that could cause a decline in RQ include a relative increase of O_2 uptake [e.g., through production of reactive oxygen species associated with cell death during the experiment (Chae & Lee, 2001)].

While not conclusive, our results suggest that the potential role of PEPC in tree roots deserves further exploration. PEPC has an important role in plant metabolism, synthesizing C_4 organic acids from HCO_3^- and phospho*enol*pyruvate (PEP). The carbon skeletons of the organic acids can be also used to generate amino acids. High activity of PEPC in roots of model plants is well documented and linked, among other factors, with exudation of organic and amino acids to the rhizosphere (Neumann & Römheld, 2007; O'Leary, Park, & Plaxton, 2011). The addition of Δ_R and RQ analysis to the PEPC assessments toolbox that contains enzymatic and genetic assays can provide realistic estimations for the rate of PEPC activity, although this first requires resolving mixing effects on Δ_R. Compound-specific analysis (using GC-C-IRMS) for $\delta^{13}C$ of the putative respiratory substrates and metabolites might provide more accurate Δ_R values and information about PEPC metabolism.

ACKNOWLEDGMENTS

We thank Axel Steinhof and Heike Machts for processing and measuring the radiocarbon samples, Heiko Moossen, Petra Linke and Heike Geilmann for processing and measuring the $\delta^{13}C$ samples, Stephanie Strahl for helping with NSC extractions and Anette Enke for HPLC measurements. Funding: The Max Planck Institute for Biogeochemistry and the European Research Council Horizon 2020 Research and Innovation Programme, grant agreement 695101 (14Constraint). Jan Muhr received funding from the European Research Council under the European Research Council Horizon 2020 Research and Innovation Programme, grant agreement 682512 (OXYFLUX).

CONFLICT OF INTEREST

The authors declare no conflict of interest.

DATA AVAILABILITY STATEMENT

The data that support the findings of this study are openly available in 'Zenodo' at https://doi.org/10.5281/zenodo.4281013, and in the supplementary material of this article.

ORCID

Boaz Hilman https://orcid.org/0000-0003-3403-1561

REFERENCES

Badeck, F. W., Tcherkez, G., Nogues, S., Piel, C., & Ghashghaie, J. (2005). Post-photosynthetic fractionation of stable carbon isotopes between plant organs- a widespread phenomenon. *Rapid Communications in Mass Spectrometry*, *19*(11), 1381–1391. https://doi.org/10.1002/rcm.1912

Bastos, A., Ciais, P., Friedlingstein, P., Sitch, S., Pongratz, J., Fan, L., … Zaehle, S. (2020). Direct and seasonal legacy effects of the 2018 heat wave and drought on European ecosystem productivity. *Science Advances*, *6*(24), eaba2724. https://doi.org/10.1126/sciadv.aba2724

Bathellier, C., Tcherkez, G., Bligny, R., Gout, E., Cornic, G., & Ghashghaie, J. (2009). Metabolic origin of the $\delta^{13}C$ of respired CO_2 in roots of *Phaseolus vulgaris*. *The New Phytologist*, *181*(2), 387–399. https://doi.org/10.1111/j.1469-8137.2008.02679.x

Bouriaud, O., Marin, G., Bouriaud, L., Hessenmoller, D., & Schulze, E. D. (2016). Romanian legal management rules limit wood production in Norway spruce and beech forests. *Forest Ecosystems*, *3*(1), 20. https://doi.org/10.1186/s40663-016-0079-2

Bowling, D. R., Pataki, D. E., & Randerson, J. T. (2008). Carbon isotopes in terrestrial ecosystem pools and CO_2 fluxes. *The New Phytologist*, *178*(1), 24–40. https://doi.org/10.1111/j.1469-8137.2007.02342.x

Brown, S. E., Pregitzer, K. S., Reed, D. D., & Burton, A. J. (2000). Predicting daily mean soil temperature from daily mean air temperature in four northern hardwood forest stands. *Forest Science*, *46*(2), 297–301. https://doi.org/10.1093/forestscience/46.2.297

Brugnoli, E., Hubick, K. T., von Caemmerer, S., Wong, S. C., & Farquhar, G. D. (1988). Correlation between the carbon isotope discrimination in leaf starch and sugars of C3 plants and the ratio of intercellular and atmospheric partial pressures of carbon dioxide. *Plant Physiology*, *88*(4), 1418–1424. https://doi.org/10.1104/pp.88.4.1418

Burton, A. J., & Pregitzer, K. S. (2003). Field measurements of root respiration indicate little to no seasonal temperature acclimation for sugar maple and red pine. *Tree Physiology*, *23*(4), 273–280. https://doi.org/10.1093/treephys/23.4.273

Carbone, M. S., Czimczik, C. I., Keenan, T. F., Murakami, P. F., Pederson, N., Schaberg, P. G., … Richardson, A. D. (2013). Age, allocation and availability of nonstructural carbon in mature red maple trees. *The New Phytologist*, *200*(4), 1145–1155. https://doi.org/10.1111/nph.12448

Chae, H. S., & Lee, W. S. (2001). Ethylene- and enzyme-mediated superoxide production and cell death in carrot cells grown under carbon

starvation. *Plant Cell Reports*, *20*(3), 256–261. https://doi.org/10.1007/s002990000307

Chapin, F. S., III, Schulze, E., & Mooney, H. A. (1990). The ecology and economics of storage in plants. *Annual Review of Ecology and Systematics*, *21*(1), 423–447. https://doi.org/10.1146/annurev.es.21.110190.002231

Ciais, P., Sabine, C., Bala, G., Bopp, L., Brovkin, V., Canadell, J., … Zeng, N. (2014). Carbon and Other Biogeochemical Cycles. Retrieved from https://www.ipcc.ch/site/assets/uploads/2018/02/WG1AR5_Chapter06_FINAL.pdf

Damesin, C., & Lelarge, C. (2003). Carbon isotope composition of current-year shoots from *Fagus sylvatica* in relation to growth, respiration and use of reserves. *Plant, Cell & Environment*, *26*(2), 207–219. https://doi.org/10.1046/j.1365-3040.2003.00951.x

Dietze, M. C., Sala, A., Carbone, M. S., Czimczik, C. I., Mantooth, J. A., Richardson, A. D., & Vargas, R. (2014). Nonstructural carbon in woody plants. *Annual Review of Plant Biology*, *65*, 667–687. https://doi.org/10.1146/annurev-arplant-050213-040054

Epron, D., Ngao, J., Dannoura, M., Bakker, M. R., Zeller, B., Bazot, S., … Loustau, D. (2011). Seasonal variations of belowground carbon transfer assessed by in situ $^{13}CO_2$ pulse labelling of trees. *Biogeosciences*, *8*(5), 1153–1168. https://doi.org/10.5194/bg-8-1153-2011

Farquhar, G. D., Oleary, M. H., & Berry, J. A. (1982). On the relationship between carbon isotope discrimination and the inter-cellular carbon-dioxide concentration in leaves. *Australian Journal of Plant Physiology*, *9*(2), 121–137. https://doi.org/10.1071/Pp9820121

Farquhar, G. D., & Sharkey, T. D. (1982). Stomatal conductance and photosynthesis. *Annual Review of Plant Physiology and Plant Molecular Biology*, *33*(1), 317–345. https://doi.org/10.1146/annurev.pp.33.060182.001533

Fischer, S., Hanf, S., Frosch, T., Gleixner, G., Popp, J., Trumbore, S., & Hartmann, H. (2015). *Pinus sylvestris* switches respiration substrates under shading but not during drought. *The New Phytologist*, *207*(3), 542–550. https://doi.org/10.1111/nph.13452

Fraser, E. C., Lieffers, V. J., & Landhausser, S. M. (2006). Carbohydrate transfer through root grafts to support shaded trees. *Tree Physiology*, *26*(8), 1019–1023. https://doi.org/10.1093/treephys/26.8.1019

Furze, M. E., Huggett, B. A., Chamberlain, C. J., Wieringa, M. M., Aubrecht, D. M., Carbone, M. S., … Richardson, A. D. (2020). Seasonal fluctuation of nonstructural carbohydrates reveals the metabolic availability of stemwood reserves in temperate trees with contrasting wood anatomy. *Tree Physiology*, *40*(10), 1355–1365. https://doi.org/10.1093/treephys/tpaa080

Gaspard, D. T., & DesRochers, A. (2020). Natural root grafting in hybrid poplar clones. *Trees-Structure and Function*, *34*(4), 881–890. https://doi.org/10.1007/s00468-020-01966-z

Gaudinski, J. B., Torn, M., Riley, W., Dawson, T., Joslin, J., & Majdi, H. (2010). Measuring and modeling the spectrum of fine-root turnover times in three forests using isotopes, minirhizotrons, and the radix model. *Global Biogeochemical Cycles*, *24*(3). https://doi.org/10.1029/2009GB003649

Gessler, A., Keitel, C., Kodama, N., Weston, C., Winters, A. J., Keith, H., … Farquhar, G. D. (2007). $\delta^{13}C$ of organic matter transported from the leaves to the roots in *Eucalyptus delegatensis*: Short-term variations and relation to respired CO_2. *Functional Plant Biology*, *34*(8), 692–706. https://doi.org/10.1071/FP07064

Ghashghaie, J., & Badeck, F. W. (2014). Opposite carbon isotope discrimination during dark respiration in leaves versus roots - a review. *The New Phytologist*, *201*(3), 751–769. https://doi.org/10.1111/nph.12563

Ghashghaie, J., Badeck, F. W., Lanigan, G., Nogués, S., Tcherkez, G., Deléens, E., … Griffiths, H. (2003). Carbon isotope fractionation during dark respiration and photorespiration in C_3 plants. *Phytochemistry Reviews*, *2*(1-2), 145–161. https://doi.org/10.1023/B:PHYT.0000004326.00711.ca

Gleixner, G., Danier, H. J., Werner, R. A., & Schmidt, H. L. (1993). Correlations between the ^{13}C content of primary and secondary plant products in different cell compartments and that in decomposing Basidiomycetes. *Plant Physiology*, *102*(4), 1287–1290. https://doi.org/10.1104/pp.102.4.1287

Herrera-Ramirez, D., Muhr, J., Hartmann, H., Romermann, C., Trumbore, S., & Sierra, C. A. (2020). Probability distributions of non-structural carbon ages and transit times provide insights into carbon allocation dynamics of mature trees. *The New Phytologist*, *226*(5), 1299–1311. https://doi.org/10.1111/nph.16461

Hilman, B., Muhr, J., Trumbore, S. E., Kunert, N., Carbone, M. S., Yuval, P., … Angert, A. (2019). Comparison of CO_2 and O_2 fluxes demonstrate retention of respired CO_2 in tree stems from a range of tree species. *Biogeosciences*, *16*(1), 177–191. https://doi.org/10.5194/bg-16-177-2019

Hoper, S. T., McCormac, F. G., Hogg, A. G., Higham, T. F. G., & Head, M. J. (2016). Evaluation of wood pretreatments on oak and cedar. *Radiocarbon*, *40*(1), 45–50. https://doi.org/10.1017/s0033822200017860

Hua, Q., Barbetti, M., & Rakowski, A. Z. (2016). Atmospheric radiocarbon for the period 1950–2010. *Radiocarbon*, *55*(4), 2059–2072. https://doi.org/10.2458/azu_js_rc.v55i2.16177

Jackson, R. B., Mooney, H. A., & Schulze, E. D. (1997). A global budget for fine root biomass, surface area, and nutrient contents. *Proceedings of the National Academy of Sciences of the United States of America*, *94*(14), 7362–7366. https://doi.org/10.1073/pnas.94.14.7362

Kodama, N., Barnard, R. L., Salmon, Y., Weston, C., Ferrio, J. P., Holst, J., … Gessler, A. (2008). Temporal dynamics of the carbon isotope composition in a *Pinus sylvestris* stand: From newly assimilated organic carbon to respired carbon dioxide. *Oecologia*, *156*(4), 737–750. https://doi.org/10.1007/s00442-008-1030-1

Kudsk, S. G., Olsen, J., Nielsen, L. N., Fogtmann-Schulz, A., Knudsen, M. F., & Karoff, C. (2018). What is the carbon origin of early-wood? *Radiocarbon*, *60*(5), 1457–1464. https://doi.org/10.1017/RDC.2018.97

Lacointe, A., Kajji, A., Daudet, F. A., Archer, P., & Frossard, J. S. (1993). Mobilization of carbon reserves in young walnut trees. *Acta Botanica Gallica*, *140*(4), 435–441. https://doi.org/10.1080/12538078.1993.10515618

Landhausser, S. M., Chow, P. S., Dickman, L. T., Furze, M. E., Kuhlman, I., Schmid, S., … Adams, H. D. (2018). Standardized protocols and procedures can precisely and accurately quantify non-structural carbohydrates. *Tree Physiology*, *38*(12), 1764–1778. https://doi.org/10.1093/treephys/tpy118

Levin, I., & Hesshaimer, V. (2016). Radiocarbon – A unique tracer of global carbon cycle dynamics. *Radiocarbon*, *42*(1), 69–80. https://doi.org/10.1017/s0033822200053066

Levy-Varon, J. H., Schuster, W. S., & Griffin, K. L. (2012). The autotrophic contribution to soil respiration in a northern temperate deciduous forest and its response to stand disturbance. *Oecologia*, *169*(1), 211–220. https://doi.org/10.1007/s00442-011-2182-y

Litton, C. M., Raich, J. W., & Ryan, M. G. (2007). Carbon allocation in forest ecosystems. *Global Change Biology*, *13*(10), 2089–2109. https://doi.org/10.1111/j.1365-2486.2007.01420.x

Madhavan, S., Treichel, I., & Oleary, M. H. (1991). Effects of relative-humidity on carbon isotope fractionation in plants. *Botanica Acta*, *104*(4), 292–294. https://doi.org/10.1111/j.1438-8677.1991.tb00232.x

Masiello, C. A., Gallagher, M. E., Randerson, J. T., Deco, R. M., & Chadwick, O. A. (2008). Evaluating two experimental approaches for measuring ecosystem carbon oxidation state and oxidative ratio. *Journal of Geophysical Research – Biogeosciences*, *113*(G3). https://doi.org/10.1029/2007JG000534

Maunoury-Danger, F., Fresneau, C., Eglin, T., Berveiller, D., Francois, C., Lelarge-Trouverie, C., & Damesin, C. (2010). Impact of carbohydrate supply on stem growth, wood and respired CO_2 $\delta^{13}C$: Assessment by

experimental girdling. *Tree Physiology*, *30*(7), 818–830. https://doi.org/10.1093/treephys/tpq039

Mudge, K., Janick, J., Scofield, S., & Goldschmidt, E. E. (2009). A history of grafting. doi: https://doi.org/10.1002/9780470593776.ch9

Muhr, J., Trumbore, S., Higuchi, N., & Kunert, N. (2018). Living on borrowed time - Amazonian trees use decade-old storage carbon to survive for months after complete stem girdling. *The New Phytologist*, *220*(1), 111–120. https://doi.org/10.1111/nph.15302

Neumann, G., & Römheld, V. (2007). The release of root exudates as affected by the plant physiological status. In R. Pinton, Z. Varanini, & Z. Nannipieri (Eds.), *The Rhizosphere: Biochemistry and organic substances at the soil-plant interface* (2nd ed., pp. 23–72). Boca Raton, Florida: CRC Press.

O'Leary, B., Park, J., & Plaxton, W. C. (2011). The remarkable diversity of plant PEPC (phospho*enol*pyruvate carboxylase): Recent insights into the physiological functions and post-translational controls of non-photosynthetic PEPCs. *Biochemical Journal*, *436*(1), 15–34. https://doi.org/10.1042/BJ20110078

Pate, J., & Arthur, D. (1998). $\delta^{13}C$ analysis of phloem sap carbon: Novel means of evaluating seasonal water stress and interpreting carbon isotope signatures of foliage and trunk wood of *Eucalyptus globulus*. *Oecologia*, *117*(3), 301–311. https://doi.org/10.1007/s004420050663

Pilcher, J. R. (1995). Biological considerations in the interpretation of stable isotope ratios in oak tree-rings. *Paläoklimaforschung*, *15*, 157–161.

Pregitzer, K. S., & Friend, A. L. (1996). The structure and function of *Populus* root systems. In R. Stettler, T. Bradshaw, P. Heilman, & T. Hinckley (Eds.), *Biology of Populus and its implications for management and conservation* (pp. 331–354). Ottawa, ON: NRC Research Press.

Pregitzer, K. S., Laskowski, M. J., Burton, A. J., Lessard, V. C., & Zak, D. R. (1998). Variation in sugar maple root respiration with root diameter and soil depth. *Tree Physiology*, *18*(10), 665–670. https://doi.org/10.1093/treephys/18.10.665

R Core Team. (2019). R: A Language and Environment for Statistical Computing. Retrieved from https://www.R-project.org/

Raessler, M., Wissuwa, B., Breul, A., Unger, W., & Grimm, T. (2010). Chromatographic analysis of major non-structural carbohydrates in several wood species - an analytical approach for higher accuracy of data. *Analytical Methods*, *2*(5), 532–538. https://doi.org/10.1039/B9AY00193J

Richardson, A. D., Carbone, M. S., Huggett, B. A., Furze, M. E., Czimczik, C. I., Walker, J. C., … Murakami, P. (2015). Distribution and mixing of old and new nonstructural carbon in two temperate trees. *The New Phytologist*, *206*(2), 590–597. https://doi.org/10.1111/nph.13273

Richardson, A. D., Carbone, M. S., Keenan, T. F., Czimczik, C. I., Hollinger, D. Y., Murakami, P., … Xu, X. (2013). Seasonal dynamics and age of stemwood nonstructural carbohydrates in temperate forest trees. *The New Phytologist*, *197*(3), 850–861. https://doi.org/10.1111/nph.12042

Rog, I., Rosenstock, N. P., Korner, C., & Klein, T. (2020). Share the wealth: Trees with greater ectomycorrhizal species overlap share more carbon. *Molecular Ecology*, *29*(13), 2321–2333. https://doi.org/10.1111/mec.15351

Scartazza, A., Moscatello, S., Matteucci, G., Battistelli, A., & Brugnoli, E. (2015). Combining stable isotope and carbohydrate analyses in phloem sap and fine roots to study seasonal changes of source-sink relationships in a Mediterranean beech forest. *Tree Physiology*, *35*(8), 829–839. https://doi.org/10.1093/treephys/tpv048

Steinhof, A., Altenburg, M., & Machts, H. (2017). Sample preparation at the Jena ^{14}C laboratory. *Radiocarbon*, *59*(3), 815–830. https://doi.org/10.1017/rdc.2017.50

Tcherkez, G., Nogues, S., Bleton, J., Cornic, G., Badeck, F., & Ghashghaie, J. (2003). Metabolic origin of carbon isotope composition of leaf dark-respired CO_2 in French bean. *Plant Physiology*, *131*(1), 237–244. https://doi.org/10.1104/pp.013078

Trumbore, S., Czimczik, C. I., Sierra, C. A., Muhr, J., & Xu, X. (2015). Nonstructural carbon dynamics and allocation relate to growth rate and leaf habit in California oaks. *Tree Physiology*, *35*(11), 1206–1222. https://doi.org/10.1093/treephys/tpv097

Trumbore, S., Sierra, C., & Pries, C. H. (2016). Radiocarbon nomenclature, theory, models, and interpretation: Measuring age, determining cycling rates, and tracing source pools. In *Radiocarbon and climate change* (pp. 45–82). Cham, Switzerland: Springer.

Wendeberg, M., Richter, J. M., Rothe, M., & Brand, W. A. (2013). Jena reference air set (JRAS): A multi-point scale anchor for isotope measurements of CO_2 in air. *Atmospheric Measurement Techniques*, *6*(3), 817–822. https://doi.org/10.5194/amt-6-817-2013

Werner, C., & Gessler, A. (2011). Diel variations in the carbon isotope composition of respired CO_2 and associated carbon sources: A review of dynamics and mechanisms. *Biogeosciences*, *8*(9), 2437–2459. https://doi.org/10.5194/bg-8-2437-2011

SUPPORTING INFORMATION

Additional supporting information may be found online in the Supporting Information section at the end of this article.

How to cite this article: Hilman, B., Muhr, J., Helm, J., Kuhlmann, I., Schulze, E.-D., & Trumbore, S. (2021). The size and the age of the metabolically active carbon in tree roots. *Plant, Cell & Environment*, 1–14. https://doi.org/10.1111/pce.14124